Journal for ImmunoTherapy of Cancer

Scalable generation of functional human iPSC-derived CAR-macrophages that efficiently eradicate CD19-positive leukemia

Shifaa M. Abdin,[1,2] Daniela Paasch ,[1,2] Arnold Kloos,[3] Marco Carvalho Oliveira,[1,2] Mi-Sun Jang,[1,2] Mania Ackermann,[1,4] Andriana Stamopoulou,[5] Philipp J Mroch,[4] Christine S Falk,[6] Constantin S von Kaisenberg,[7] Axel Schambach,[2,5,8] Michael Heuser,[3] Thomas Moritz,[5] Gesine Hansen,[1,9] Michael Morgan,[2,5] Nico Lachmann [1,2,4,9]

To cite: Abdin SM, Paasch D, Kloos A, *et al*. Scalable generation of functional human iPSC-derived CAR-macrophages that efficiently eradicate CD19-positive leukemia. *Journal for ImmunoTherapy of Cancer* 2023;**11**:e007705. doi:10.1136/jitc-2023-007705

► Additional supplemental material is published online only. To view, please visit the journal online (http://dx.doi.org/10.1136/jitc-2023-007705).

SMA and DP contributed equally.

MM and NL are joint senior authors.

Accepted 04 December 2023

For numbered affiliations see end of article.

Correspondence to
Dr Nico Lachmann; lachmann.nico@mh-hannover.de

ABSTRACT

Background Macrophages have recently become attractive therapeutics in cancer immunotherapy. The potential of macrophages to infiltrate and influence solid malignancies makes them promising targets for the chimeric antigen receptor (CAR) technology to redirect their stage of polarization, thus enhancing their anticancer capacities. Given the emerging interest for CAR-macrophages, generation of such cells so far mainly depends on peripheral blood monocytes, which are isolated from the respective donor prior to genetic manipulation. This procedure is time-intensive and cost-intensive, while, in some cases, insufficient monocyte amounts can be recovered from the donor, thus hampering the broad applicability of this technology. Hence, we demonstrate the generation and effectiveness of CAR-macrophages from various stem cell sources using also modern upscaling technologies for next generation immune cell farming.

Methods Primary human hematopoietic stem and progenitor cells and induced pluripotent stem cells were used to derive anti-CD19 CAR-macrophages. Anticancer activity of the cells was demonstrated in co-culture systems, including primary material from patients with leukemia. Generation of CAR-macrophages was facilitated by bioreactor technologies and single-cell RNA (scRNA) sequencing was used to characterize in-depth response and behavior of CAR-macrophages.

Results Irrespective of the stem-cell source, CAR-macrophages exhibited enhanced and antigen-dependent phagocytosis of CD19$^+$ target cancer cells with increased pro-inflammatory responses. Phagocytic capacity of CAR-macrophages was dependent on target cell CD19 expression levels with superior function of CAR-macrophages against CD19$^+$ cancer cell lines and patient-derived acute lymphocytic leukemia cancer cells. scRNA sequencing revealed CAR-macrophages to be distinct from eGFP control cells after co-culture with target cells, which includes the activation of pro-inflammatory pathways and upregulation of chemokines and cytokines associated with adaptive immune cell recruitment, favoring the repolarization of CAR-macrophages to a pro-inflammatory state. Taken together, the data highlight the unique features of CAR-macrophages in combination with the successful upscaling of the production pipeline

WHAT IS ALREADY KNOWN ON THIS TOPIC

⇒ Macrophages are among the critical innate immune cells regulating the tumor microenvironment. Macrophages equipped with chimeric antigen receptors (CARs) have been introduced as a potent cell-based immunotherapy. However, genetic engineering and manufacturing of macrophages in scalable quantities especially from human induced pluripotent stem cells (iPSC) is still a major challenge.

WHAT THIS STUDY ADDS

⇒ We introduce a modern genetic engineering approach to maintain the expression of CARs in human macrophages derived from iPSC, targeting CD19$^+$ patient-derived acute lymphocytic leukemia cancer cells.

⇒ To circumvent lack of therapeutic macrophages, we demonstrate the use of intermediate scale bioreactors and continuous production of CAR-iMacs to sufficiently eliminate CD19$^+$ target cells.

⇒ For the mode of action, single-cell RNA sequencing data revealed a sustained pro-inflammatory signature in CAR-iMacs highlighted by upregulation of interferon signaling, antigen presentation, and adaptive immune cell activation.

HOW THIS STUDY MIGHT AFFECT RESEARCH, PRACTICE OR POLICY

⇒ Our study highlights the potential to facilitate the clinical access to CAR-macrophage therapeutics, employing human iPSCs with a state-of-the-art upscaling manufacturing technique. The study lays the foundation for on-demand production of therapeutically active CAR-macrophages and paves the way for unique approaches to enhance the antitumor activity of macrophages, all dedicated to patients suffering from solid and liquid malignancies.

using a three-dimensional differentiation protocol and intermediate scale bioreactors.

Conclusion In summary, our work provides insights into the seminal use and behavior of CAR-macrophages which are derived from various sources of stem cells, while introducing a unique technology for CAR-macrophage manufacturing, all dedicated to the clinical translation of CAR-macrophages within the field of anticancer immunotherapies.

INTRODUCTION

Cancer immunotherapy has achieved remarkable success and became the fourth cornerstone in anticancer therapy after chemotherapy, surgery, and radiation. Among the recent promising approaches, adoptive cell therapies of immune cells equipped with chimeric antigen receptors (CARs) have gained increased attention. In fact, CAR-T cell therapy is now in clinical practice with six regulatory agency-approved therapies.[1] Similarly, there are multiple clinical trials ongoing, exploring the potential of CAR-natural killer cells in targeting different hematological and solid malignancies.[2 3] However, both cell types have made poor progression in targeting solid tumors due to the limited efficiency against the immune-inhibitory tumor microenvironment (TME) and low trafficking and infiltration rate to the solid tumor bed.[4 5]

CAR-macrophages have emerged as a promising alternative. With their well-known capacity to infiltrate the solid tumor, macrophages are considered as a suitable cell type for anticancer therapy.[6 7] Several groups have shown encouraging in vitro and in vivo results with CAR-macrophages against both hematological and solid malignancies targeting breast and ovarian cancer.[8–10] Currently, one CAR-macrophage candidate against HER2-positive breast cancer is in a phase I clinical trial (NCT04660929). Still, the clinical translation of this approach is hampered by the low yields of patient monocytes and insufficient ex vivo expansion techniques. Additionally, genetic engineering of CAR-macrophages is of limited efficiency in primary monocytes given their resistance to lentiviral transduction, while adenoviral delivery cannot maintain long-term transgene expression.[1] Besides attempts to genetically manipulate macrophages directly in vivo, other cell sources of human monocyte/macrophages are of great interest and could further facilitate the clinical translation of these cells.

In this line, human induced pluripotent stem cells (hiPSC), with their unlimited proliferation and differentiation potential, serve as an attractive platform for upscaled production of genetically-engineered hematopoietic immune cells, providing CAR-macrophages as a readily available off-the shelf immune-based therapy. Successful generation of human macrophages from iPSCs (iMacs) was previously shown, demonstrating iMacs to be phenotypically, functionally and transcriptionally similar to primary monocyte-derived macrophages.[11–13] Given these similarities, iMacs were frequently used to gain insights into the pathophysiology of different diseases, while the feasibility to derive iMacs by unique differentiation techniques could facilitate development of novel immunotherapies for the lung, brain or liver. iMacs also have the capacity to react to certain (tissue) environments, which can define the stage of activation. Furthermore, strong anti-inflammatory and pro-inflammatory cues have been applied to iMacs, demonstrating the unique re-polarizing feature of these cells. Given the promising attempts to use CAR-macrophages in modern cell-based immunotherapies, insights into the overall behavior of CAR-macrophages and the feasibility to derive scalable numbers are of utmost need to broaden the use of this technology.

In our study, we aimed to combine the CAR technology with a seminal technology to derive iPSC-macrophages in scalable quantities. Proof-of-concept for an anti-CD19 CAR construct was first performed using primary hematopoietic stem and progenitor cells (HSPCs). Translation into the iPSC-based system and the continuous and scalable differentiation technique was used to assess the beneficial use of CAR-iMacs against different $CD19^+$ target cells, includingt primary acute lymphocytic leukemia (ALL) samples. Unique insights into the specificity of the CAR construct and the instructive potential to induce a pro-inflammatory signature within CAR-iMacs were revealed by single-cell RNA (scRNA) sequencing, which provided new insights into the mechanism of the frequently used FcRγ signaling domain, highlighting the broad applicability of iMacs as suitable cells for genetic modifications with various cancer cell-targeting CARs.

MATERIALS AND METHODS

Generation of αCD19 CAR constructs and lentiviral vector production

The SFFV_ΔCAR and SFFV_CAR vectors were purchased from Addgene (#113014 and #113019). To generate the CBX3.EFS.CAR vector, the CAR sequence from the SFFV_CAR vector was cloned into a third generation self-inactivating (SIN) lentiviral backbone (pRRL.cPPT.CBX3.EFS) using flanking restriction sites. Subsequently, an Internal ribosome entry site (IRES) coupled to enhanced green fluorescent protein (eGFP) reporter sequence was inserted into the *SalI* site of the pRRL.cPPT.CBX3.EFS.CAR vector. The engineered CBX3.EFS.CAR vector was then verified via DNA sequencing (GATC and SeqLab). The eGFP control vector (pRRL.cPPT.CAG.iGFP) was kindly provided by Dr Malte Sgodda and the mCherry-expressing vector (Addgene #27339) by Professor Boris Fehse (UKE Hamburg). The detailed process of lentiviral vector production was performed as previously described.[14]

$CD34^+$ cell isolation from cord blood

Umbilical cord blood was collected from healthy donors after obtaining signed informed consent, in cooperation with the Department of Gynecology and Prenatal Medicine (Hannover Medical School) and in line with the standards of the Hannover Medical School Ethics Committee (protocol code 1303–2012). Briefly, peripheral blood

mononuclear cells (PBMCs) were isolated using a BioColl density gradient centrifugation, followed by $CD34^+$ cell enrichment using a bead-conjugated anti-CD34 antibody (Miltenyi, Germany) for magnetic cell separation. $CD34^+$ cells were cultured in StemSpan medium (STEMCELL Technologies, Vancouver, Canada) containing 1 mM penicillin–streptomycin (P/S), 2 mM L-glutamine (L-Glu), 100 ng/mL human stem cell factor (hSCF), 100 ng/mL FMS-like tyrosine kinase3 ligand (hFlt3L) and 50 ng/mL human thrombopoietin (hTPO) (PeproTech, Rocky Hill, USA), further details can be found in the previous published work.[14]

Transduction of cord blood-derived $CD34^+$ cells and differentiation to macrophages

24 hours post-isolation, 2×10^5 freshly-isolated cord blood-derived $CD34^+$ cells were transduced with a multiplicity of infection (MOI) of 5 and further sorted and differentiated into mature macrophages as shown in detail in a previous study.[14]

iPS cell cultivation and differentiation to macrophages

iPSC cultivation was performed using a feeder-free protocol. iPSC cells were cultured on Geltrex-coated tissue culture plates or T25 flasks using E8 medium (containing DMEM/F-12 (Gibco, Life Technologies), 64 mg/L ascorbic acid 2-phosphate, 14 µg/L sodium selenite, 543 mg/L, $NaHCO_3$ and 20 mg/L insulin, and 10,7 mg/L human recombinant transferrin (all from Sigma-Aldrich) supplemented with 100 ng/mL human basic fibroblast growth factor (hbFGF) and 2 ng/mL human transforming growth factor beta (TGFß) (both from PeproTech) under standard humidified conditions at 37°C and 5% CO_2. The cells were split two times a week using Accutase (STEMCELL Technologies) and under the addition of 10 µM ROCK inhibitor (RI; Tocris, Bristol, UK). A complete medium change using ROCK inhibitor-free medium was performed 48 hours after splitting. In order to start mesoderm priming, 5×10^5 iPS cells were seeded in 3 mL of mesoderm priming I medium (E8 medium supplemented with 10 µM RI, 50 ng/mL human vascular endothelial growth factor (hVEGF) and human bone morphogenetic protein 4 (hBMP4) and 20 ng/mL hSCF (all from PeproTech) using CELLSTAR 6-well plates placed on an orbital shaker at 70 rpm, leading to the formation of embryoid bodies (EBs). On day 2, the medium was changed to E6 medium (containing only hVEGF, hBMP4 and hSCF) . On day 4 after mesoderm priming I, supernatant was discarded and 3 mL of mesoderm priming II medium (E6 medium supplemented with 50 ng/mL hVEGF and hBMP4, 20 ng/mL hSCF and 25 ng/mL human interleukin 3(hIL-3)) was added, while increasing the shaking speed to 85 rpm. Mesoderm priming medium II was refreshed at day 7 before macrophage differentiation (hematopoietic differentiation) was started at day 10. For this, the medium was removed and the EBs were transferred to a 6-well tissue culture plate using 2 mL of differentiation medium (X-VIVO containing 1% (v/v) P/S and L-Glu, 0.1% (v/v) β-mercaptoethanol supplemented with 25 ng/mL hIL-3 and 50 ng/mL human macrophage colony stimulating factor (hM-CSF). Macrophage production started from day 4 onwards and can be continuously harvested 1–2×per week. The harvested macrophages were filtered (70 µM pore size) and seeded in Roswell Park Memorial Institute (RPMI1640) medium containing 1% (v/v) P/S, 10% (v/v) fetal bovine serum (FBS) and 50 ng/mL hM-CSF using tissue culture plates.

Transduction of iPS cells with lentiviral vectors

8×10^4 iPSCs were seeded on Geltrex-coated 12-well plates in E8 medium under the addition of 10 µM ROCK inhibitor (RI). At 80% confluency, iPS cells were transduced with an MOI of 5 using E8 medium supplemented with 4 µg/mL of protamine sulfate in a total volume of 500 µL. 24 hours post-transduction, 1 mL E8 medium was added and after an additional of 24 hours, total medium change was performed. 4 days post-transduction, cells were detached using Accutase and transferred to a new Geltrex-coated 6-well plate for further expansion.

Cancer cell line culture conditions

RAJI, K562 and DAUDI cells were cultured in RPMI 1640 medium containing 10% (v/v) FBS and 1 % P/S (v/v) using 12-well suspension plates. All cell lines were cultured under standard humidified conditions at 37°C and 5% CO_2 and split two times a week in a 1:10 ratio.

Transduction of cancer cell lines with a lentiviral mCherry construct

4×10^5 cells were transduced with an MOI of 1 using the standard culture medium containing 4 µg/mL of protamine sulfate. 48 hours post-transduction, the cells were washed and seeded back. To determine the transduction efficiency 96 hours post-transduction, flow cytometric analysis was performed detecting mCherry expression.

Cultivation of $CD19^+$ patient with ALL samples

Patient samples were collected after obtaining informed consents, aligned with the approval of the local ethical committee (666/2010). The primary patient ALL cells were cultured in Iscove's Modified Dulbecco's Medium (IMDM; Gibco, Life Technologies) containing 20% (v/v) BIT (STEMCELL Technologies), 1% (v/v) P/S and L-Glu and 0.1 mM β-mercaptoethanol (supplemented with 20 ng/mL hIL-6, hIL-3 and human granulocyte colony stimulating factor (hG-CSF), 50 ng/mL hTPO and 100 ng/mL hFlt3L and hSCF) using 6-well suspension plates. 48 hours post-thawing, the cells were used for co-culture experiments. For detection of the ALL cancer cells in the co-culture set-up, the ALL cells were prestained with the cell proliferation dye eFluor 670 (Invitrogen) before co-culturing them with the macrophages. Thereafter, the eFluor 670 signal acquired in the Allophycocyanin (APC) channel of the flow cytometer was quantified inside the pregated GFP^+ iMacs.

Alkaline phosphatase staining

5×10^5 anti-CD19 CAR-iPSCs were seeded on Geltrex-coated 6-well plates. When the cells reached 70% confluency, they were stained with the monolayer Alkaline Phosphatase Staining Kit II (00–0055, Stemgent, Glasgow, UK) according to the manufacturer's recommendations.

Cytospins

3×10^4 macrophages were resuspended in 150 µL phosphate-buffered saline (PBS) and centrifuged on glass slides (Menzel) using a Cytofuge (Medite) for 10 min at 700×g. Slides were stained with a 0.25% (w/v) May-Grünwald solution (Roth, Karlsruhe, Germany) for 5 min, washed thoroughly, and stained for 20 min with 1:20 diluted GIEMSA solution (Roth). The slides were washed a second round and dried over night . until coverage in Roti-Histokitt mounting solution (Roth). All images were taken with an Olympus IX71 using the CellSens Dimension imaging software (Olympus, Hamburg, Germany).

Phagocytosis assay (pHRodo)

Phagocytosis of pHrodo-coupled *Escherichia coli* particles (#P35361 Life Technologies) by macrophages was performed as described previously.[15]

Flow cytometry

To detect surface markers and reporter genes, flow cytometric analyses were performed using a CytoFLEX S flow cytometer (Beckman Coulter, Brea, California, USA) with the following antibodies: hCD45-PE-Cy7 (cat. no. 25–0459), hCD11b-APC (17-0118-41), hCD14-PE (12-0149-41), hCD163-APC (17-1639-41), hCD86-PE (12-0869-41), hCD25-Alexa Fluor 488 (53–0259) (all from eBioscience, San Diego, USA) and CD69-Pacific Blue 450 (cat. no. 310920, BioLegend, San Diego, USA). Prior to the staining procedure, cells were blocked for 5 min at room temperature (RT) with human Fc-Block TruStain FcX (BioLegend), according to the manufacturer's instructions. Data analysis was performed using FlowJo V.10.

Western blot

A minimum of 5×10^5 iMacs were collected for protein isolation using RIPA-buffer (Sigma-Aldrich) with phosphatase inhibitor (Thermo Fisher Scientific). The protein amount was quantified via BCA assay (Thermo Fisher Scientific) according to manufacturer's recommendations. CAR constructs were detected with an anti-CD8α antibody (H00000925-D01P Abnova, Thermo Scientific, Massachusetts, USA), and Vinculin (Sigma-Aldrich) was used as a loading control. After primary antibody incubation, membranes were incubated with secondary HRP-conjugated antibodies (IgG anti-Rabbit IgG-HRPO (711-035-152) and anti-Mouse IgG-HRPO (715-035-150)), (Dianova, Biozol, Hamburg, Germany). Protein bands were visualized using SuperSignal West Femto Maximum Sensitivity Substrate (Thermo Fisher Scientific).

Assessment of macrophage phagocytic capacity against cancer cells via flow cytometry

1.5×10^5 macrophages were seeded in a 12-well tissue culture plate o.n. 3 hours prior to the addition of 1.5×10^5 cancer cells (effector (E)/ target (T) ratio 1:1), macrophages were stimulated with 500 ng/mL lipopolysaccharides (LPS) (Sigma). After co-culture, supernatants and cells were collected and filtered through a 70 µM pore size filter. Adherent macrophages were washed with PBS and incubated with 500 µL Accutase for 20 min at 37°C before adding to the fluorescence-activated cell sorting (FACS) tube. Cells were centrifuged and analyzed using a CytoFLEX S or an image-based flow cytometer Flowcyte (Amnis). Phagocytic events were determined by pre-gating on the $eGFP^+$ macrophage population and analyzing the % of mCherry signal within the gate.

Assessment of macrophage phagocytic capacity against cancer cells via confocal microscopy

2×10^5 macrophages were seeded on a 12 mm round coverslip in a 24-well suspension plate using 500 µL of standard culture medium containing 100 ng/mL of hM-CSF o.n. Macrophages were stimulated with 500 ng/mL LPS (Sigma) 3 hours prior to the addition of 2×10^5 Raji cells (E:T ratio 1:1). For phagocytosis inhibition experiments, 10 µg/mL of cytochalasin D (Thermo Fisher Scientific) was added 1-hour prior to the addition of cancer cells. After 4 hours, supernatant was removed and the coverslip-containing well was carefully washed two times with 500 µL of PBS. For fixation, cells were incubated for 15 min with 500 µL of 4% paraformaldehyde(PFA) (Sigma-Aldrich, diluted in PBS). After three rounds of careful washing with 500 µL of 1×tris buffered saline (TBS) for 5 min, the coverslips were air-dried, placed onto a glass slide in an inverted manner and embedded using ProLong Gold Antifade mounting medium (Life Technologies). All images were taken using an inverted Leica TCS SP8 microscope (Leica Microsystems) with the LAS X analysis software.

Assessment of iMac response to anti-inflammatory stimuli on dexamethasone treatment

2×10^5 macrophages were seeded in a 12-well tissue culture plate. After 2 days of terminal differentiation, macrophages were stimulated with 500 ng/mL LPS (Sigma), 3 hours prior to the addition of 2×10^5 cancer cells (E:T ratio 1:1). 1 hour before the addition of target cells, 1 µg/mL dexamethasone was added. After 4 hours of co-culture, the cells were collected and stained for CD86 expression before flow cytometric analyses were performed using a CytoFLEX S flow cytometer (Beckman Coulter). Prior to the staining procedure, cells were blocked for 5 min at RT with human Fc-Block TruStain FcX (BioLegend), according to the manufacturer's instructions. Data analysis was performed using FlowJo V.10. Subsequent cytokine analysis was performed using the human tumor necrosis factor alpha (TNF-α) ELISA Ready-Set-Go!

Kits (R&D Systems) according to the manufacturer's instructions.

Assessment of antigen-specific CD19^{+} Raji cell phagocytosis in co-culture with CD19^{low} K562 cells

2×10^5 macrophages were seeded in a 12-well tissue culture plate. After 2 days of terminal differentiation, macrophages were stimulated with 500 ng/mL LPS (Sigma), 3 hours prior to the addition of 2×10^5 CD19^{+} Raji and 2×10^5 CD19^{low} K562 cancer cells. After 24 hours and 48 hours of co-culture, the cells were collected and filtered through a 70 µM pore size filter. The cell mixture was stained for CD19-PE expression for 20 min at RT before flow cytometric analyses were performed using a CytoFLEX S flow cytometer (Beckman Coulter). Prior to the staining procedure, cells were blocked for 5 min at RT with human Fc-Block TruStain FcX (BioLegend), according to the manufacturer's instructions. Data analysis was performed using FlowJo V.10.

Upscaling iPS cell differentiation to macrophages

To upscale iMac differentiation, 3×10^6 iPSCs were seeded in 18 mL of mesoderm priming I medium using a 50 mL CEROTube placed on a CERO 3D Incubator & Bioreactor (OLS, Bremen, Germany) at 80 rpm and rotation period of 2 s for the first 24 hours. On day 2, the medium was changed to E6 medium (supplemented with 10 µM RI, 50 ng/mL hVEGF and hBMP4 and 20 ng/mL hSCF) and culture was continued at 65 rpm at 4 s of rotation period. On day 4, supernatant was discarded and 40 mL of mesoderm priming II medium was added. On day 7 of mesoderm priming, hematopoietic differentiation was initiated, replacing the medium with 40 mL of iMac differentiation media as indicated above. The CEROTube was placed back into CERO 3D Incubator & Bioreactor at 80 rpm and 2 s of rotation speed. Macrophage production started from day 7 onwards and was continuously harvested every 7 days.

T-cell activation by co-culture supernatants

All experiments were performed with residual blood samples obtained from healthy platelet donors of the Hannover Medical School (MHH) Institute of Transfusion Medicine and Transplant Engineering with no signs of infection. Informed consent was obtained from all donors approved by the Ethics Committee of Hannover Medical School (ethical number: 3639_2017).

PBMCs were isolated from residual blood samples from platelet apheresis disposables used for routine collection by density gradient centrifugation. CD3^{+} T cells were enriched by magnetic cell sorting using the Pan T cell Isolation Kit, and the CD8^{+} T Cell Isolation Kit (Miltenyi Biotec, Bergisch Gladbach, Germany) according to the manufacturer's instructions. T cells were cultured in RPMI medium containing 1% (v/v) P/S, 10% (v/v) FBS and 50 units/mL interleukin (IL)-2 (PeproTech) using suspension culture plates. After 3 days of culture, 3.5×10^5 T cells were seeded in a 48-well plate and incubated for 24 hours with supernatants from a previous 4 hours co-culture of eGFP or CAR-iMacs and CD19^{+} Raji cells. As a positive control of the experiment, 3.5×10^5 T cells were stimulated using 300 units/mL IL-2 and 5 µL/well TransAct (Miltenyi) for 24 hours. Afterwards, the T cells were washed, blocked and stained for CD3, CD25 and CD69 for 20 min at RT. Flow cytometric analyses were performed using a CytoFLEX S flow cytometer (Beckman Coulter).

Cytokine secretion (ELISA)

5×10^4 macrophages were seeded in a 96-well tissue culture plate using 200 µL of standard culture medium containing 100 ng/mL of hM-CSF o.n. Macrophages were stimulated with 500 ng/mL LPS (Sigma) 3 hours prior to the addition of 5×10^4 Raji cells. After 4 hours, supernatants were collected and centrifuged for 5 min at 300×g. Additionally, to evaluate the iMacs overall functionality in response to bacterial stimulation, an alternative setting was tested where 5×10^4 macrophages were seeded in a 96-well tissue culture plate and stimulated with 500 ng/mL LPS for 24 hours. Subsequent cytokine analysis was performed using the human IL-6 and TNF-α ELISA Ready-Set-Go! Kits (R&D Systems) according to the manufacturer's instructions.

Cytokine/chemokine secretion (multiplex assay)

To determine the secretion of an array of different cytokines/chemokines, supernatants were collected from the co-cultures of CAR-iMacs or eGFP iMacs with CD19^{+} Raji cells for 4 hours, and the following cytometric bead assay was performed: the "Human M1/M2 macrophage panel" LEGENDplex Kit from BioLegend (San Diego, California, USA). The samples were used without further dilution. The assay was performed according to the manufacturer's instructions and measured using a CytoFLEX S cytometer (Beckman Coulter). Samples were analyzed using the software provided by BioLegend (Qognit) and graphs generated using GraphPad Prism V.9.

scRNA analysis

Sample preparation

iMacs and cancer target cells were co-cultured as described above for flow cytometry read-out. Subsequently, eGFP-positive cells were isolated using FACS. The FACS sorting was performed using an FACSAria Fusion flow cytometer (BD Biosciences, Franklin Lakes, New Jersey, USA).

Single-cell RNA sequencing library preparation and sequencing

The eGFP-positive cells (eGFP-iMacs+Raji, CAR-iMacs+Raji, CAR-iMacs+ALL) were isolated and processed for messenger RNA (mRNA) expression analysis library preparation using the Chromium NextGEM Single Cell 3′ Reagent Kits V.3.1 (10x Genomics), following the manufacturer's instructions (Manual Part Number CG000204 Rev B) to achieve a cell capture recovery of 4,000 cells per sample. The fragment length distribution of the generated libraries was monitored using the Bioanalyzer High Sensitivity DNA Assay (5067–4626; Agilent Technologies).

Library quantification was carried out using the Qubit dsDNA HS Assay Kit (Q32854; Thermo Fisher Scientific). Equal molar proportions of the mRNA expression libraries, constituting 27.3% of the sequencing run capacity each, were pooled accordingly. The pooled libraries were denatured with NaOH and then diluted to a final concentration of 1.8 pM, following the "Denature and Dilute Libraries Guide" (Document # 15048776 v02; Illumina). For sequencing, 1.3 mL of the denatured library pool, including 1% PhiX, was loaded onto an Illumina NextSeq550 sequencer. A high-output flowcell was used, and sequencing was performed with the following settings: 28 bp as sequence read 1, 56 bp as sequence read 2, 8 bp as index read 1, and 0 bp index read 2. The total number of clusters aimed for was 400 million (#20024906; Illumina).

Quality control and pre-processing

The sc-RNA sequencing (scRNA-seq) data from all three samples (eGFP-iMacs+Raji, CAR-iMacs+Raji, CAR-iMacs+ALL) were merged using the Seurat package (V.4.1.1).[16] Additionally, the CAR-iMac samples were merged separately. To remove potential doublets, the DoubletFinder package (V.2.0.3)[17] was used. Important parameters were used for doublet removal (pN=0.25, pK=0.01). Pre-processing of the merged scRNA-seq data followed the Seurat V.4 guided clustering tutorial. Filtering parameters were applied to remove low-quality cells and unwanted cell types. Specifically, cells with fewer than 200 genes, more than 8,000 genes, a unique molecular identifier (UMI) count over 1,000, or a mitochondrial count of 8% were excluded from downstream analysis. Moreover, non-macrophage cells and cells expressing MS4A1/CD19 were removed.

Clustering, visualization and cell characterization

Dimensionality reduction was performed to capture the key features and reduce the dimensionality of the data set. Highly variable genes were selected using the FindVariableFeatures function with default parameters. In addition, UMI counts and the percentage of mitochondrial genes were considered sources of unwanted variability and were regressed during scaling. The number of principal components was determined using the ElbowPlot function. To finalize the initial processing, Uniform Manifold Approximation and Projection (UMAP) and shared nearest neighbors were calculated using 11 dimensions.

Differential expression testing was performed using the FindAllMarkers function (only.pos=TRUE, min.pct=0.2, logfc.threshold=0.25), to identify genes that showed significant expression differences between cell clusters. The clusterProfiler package (V.4.4.4)[18] was used for functional enrichment analysis. Specifically, the enrichGO function was employed to identify enriched Gene Ontology (GO) terms in biological processes based on the top 200 differentially expressed genes.

RNA velocity

The command line tool from velocyto.R (V.0.6)[19] was employed to generate spliced and unspliced RNA expression matrices. Subsequently, scVelo (V.0.2.5)[20] was used for trajectory analysis based on RNA velocity. The scv.tl.rank_velocity_genes function was used to identify genes with significant RNA velocity changes, indicating their potential involvement in cell state transitions or trajectory dynamics.

Statistical analysis

Statistical analyses were performed using Prism V.9.0 software (GraphPad). Unless stated otherwise, one-way analysis of variance test with subsequent Tukey's post hoc testing was performed for statistical comparison between groups. Error bars indicate 95% CIs of the mean ****indicates p<0.0001 ***indicates p<0.001; **indicates p<0.01 and *indicates p<0.03.

RESULTS

CD34$^+$ cell-derived CAR-macrophages exhibit typical macrophage characteristics

To generate CAR-macrophages from human hematopoietic stem cells, we performed lentiviral transduction to modify cord blood-derived CD34$^+$ cells with a second generation CAR targeting CD19, containing a CD8a hinge and transmembrane domain and a tandem signaling domain combining the common ɣ subunit of Fc receptors and the p85 recruitment domain from CD19 (figure 1A). CAR expression was driven by an SFFV promoter, which was coupled to an eGFP reporter gene. The CAR was previously shown to enhance whole cell engulfment of leukemia cells in a murine macrophage cell line.[9] As controls, we used a truncated version of the anti-CD19 CAR (ΔCAR) that lacked the intracellular signaling domains, and macrophages expressing an eGFP vector control (eGFP). The CAR-transduced CD34$^+$ cells were sorted for eGFP expression and further differentiated into macrophages. The generated CAR-macrophages expressed typical macrophage surface markers (CD45$^+$, CD11b$^+$, CD14$^+$ and CD163$^+$) (figure 1B), had a similar level of basic phagocytic functionality of bacteria-coupled particles (figure 1C) and a similar cell morphology (figure 1D), when compared with truncated CAR and eGFP control macrophages. These data indicated that CAR expression does not interfere with the typical macrophage phenotype and basic phagocytic capacity.

CD34$^+$ cell-derived CAR-macrophages demonstrated enhanced phagocytosis and cytokine secretion upon co-culture with CD19$^+$ leukemia cells

We next validated the capability of CD34$^+$ cell-derived CAR-macrophages to target and phagocytose CD19$^+$ leukemia cells. It was previously shown that macrophages benefit from LPS prestimulation to induce efficient antitumor activity. Thus, the macrophages derived from iPSCs were prestimulated with LPS, prior to the addition of target

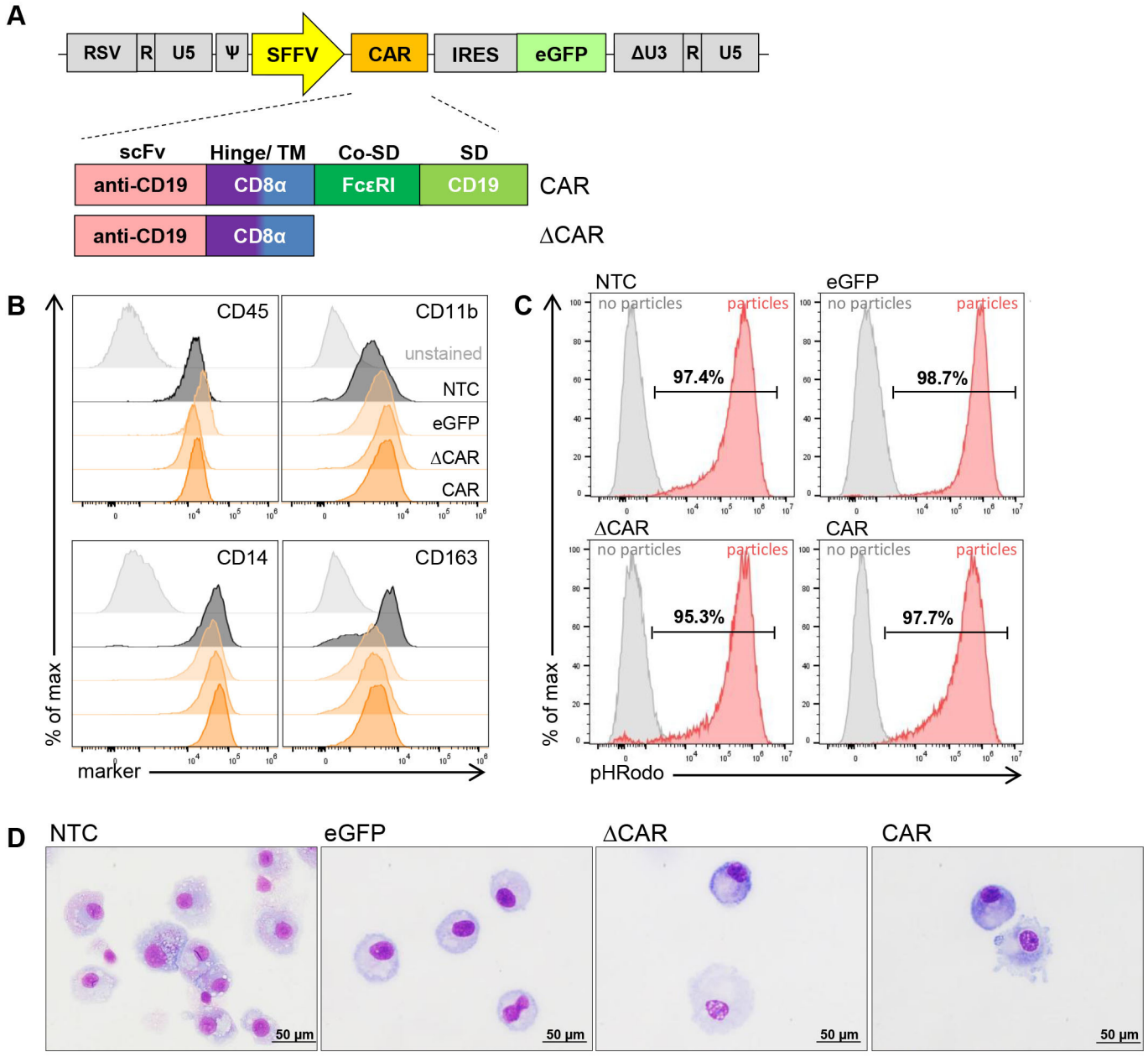

Figure 1 Characterization of cord blood-derived anti-CD19 CAR-macrophages. (A) CAR scheme depicting the composition of the anti-CD19 CAR (CAR) and the truncated version (ΔCAR) that lacks the internal signaling domain. (B) Surface marker expression profile by flow cytometric analyses. Controls include unstained control, non-transduced macrophage controls (NTC), truncated CAR-macrophages (ΔCAR) and eGFP-expressing macrophages (eGFP) (n=1). (C) Basic phagocytic activity against *Escherichia coli*-coupled particles as shown by flow cytometry (n=1). (D) Microscopic analyses of May-Grünwald-stained cytospins (using a fluorescence microscope Olympus IX71, 40× magnification, scale bar: 50 µm). CAR, chimeric antigen receptor; Co-SD, co-stimulatory signaling domain; eGFP, enhanced green fluorescent protein; IRIS,internal ribosome entery site; NTC, non-transduced control; scFv, single chain variable fragment; TM, transmembrane domain.

cells.[21] Macrophages were co-cultured with CD19$^+$ Raji cells that were engineered to express mCherry and the mCherry signal inside the CAR-macrophages was analyzed via flow cytometry. After 4 hours, eGFP macrophages, and truncated CAR-macrophages showed the lowest levels of phagocytosis (figure 2A) (23.54%±18.47%, and 33.30%±21.29%, respectively), while the highest % was demonstrated by macrophages expressing the full-length CAR (65.38%±15.82%). These results were confirmed by the quantification of mCherry signal, which also indicated the strongest phagocytic activity for macrophages carrying the full CAR (figure 2B). Further analysis of antigen-specific phagocytosis by confocal microscopy demonstrated similar results (figure 2C and online supplemental figure 1). No phagocytic events were observed for eGFP ctrl or truncated CAR-macrophages. In contrast, macrophages carrying the full-length CAR showed increased phagocytosis. In addition, preincubation of macrophages with cytochalasin D (Cyt D) demonstrated that CAR-macrophages perform an active phagocytosis, since no

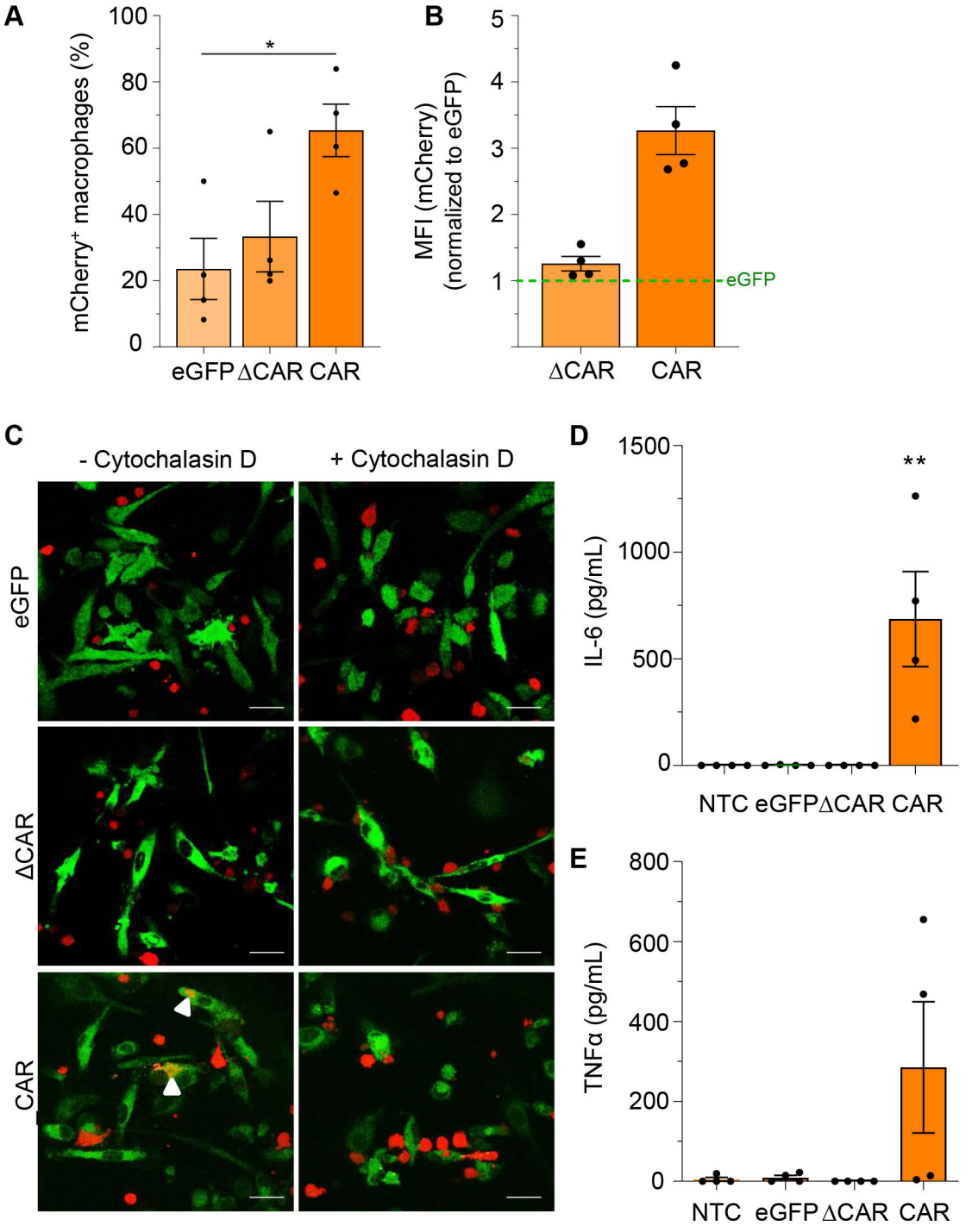

Figure 2 Evaluation of phagocytosis and cytokine secretion of cord blood-derived CAR-macrophages after co-culture with CD19+ Raji cells. Flow cytometric analysis of (A) percentage (%) of phagocytic macrophages and (B) geometric mean of mCherry signal intensity inside eGFP+ Macs after co-culture with target cells. Data are represented as the mean±SEM of n=4 biological replicates. (C) Confocal microscopy images showing phagocytosis of CD19+ Raji cells (mCherry) by macrophages (eGFP)±cytochalasin D treatment (63× oil immersion objective of the Leica DMi8 confocal microscope, scale bar: 20 µm). Secretion of (D) IL-6 and (E) TNF-α after 24 hours of co-culture of macrophages and Raji cells. Data are represented as the mean±SEM of n=4 biological replicates. Statistical significance was calculated with one-way analysis of variance using multiple comparisons. CAR, chimeric antigen receptor; eGFP enhanced green fluorescent expressing control macrophages; IL, interleukin; MFI, mean fluorescence intensity; NTC, non-transduced control; TNF, tumor necrosis factor.

phagocytic events were observed on Cyt D treatment. Analyses of IL-6 (figure 2D) and TNF-α (figure 2E) secretion from these co-cultures revealed negligible cytokine secretion from eGFP or truncated CAR-macrophages. Only the co-culture with macrophages carrying the full-length CAR showed significantly-enhanced IL-6 and increased TNF-α secretion. To exclude the risk of unspecific macrophage cross-activation, macrophages

were analyzed in mono-culture as negative controls, but only negligible cytokine expression was detected (online supplemental figure 2A and B). These data indicated CAR-specific targeting and phagocytosis of CD19$^+$ target cells, however, cytokine secretion is dependent on intracellular CAR signaling domains for proper macrophage activation.

Continuous generation of functional and mature CAR-iMacs from hiPSCs

To transfer the anti-CD19 CAR construct to hiPSCs, the previously used CAR was subcloned into a third generation SIN lentiviral construct with a CBX3-EFS promoter (figure 3A). Next, hiPSCs were transduced with the CAR or an eGFP control vector (figure 3B). Lentiviral transduction had no effect on iPSC pluripotency and differentiation capacity, as the cells showed typical expression of pluripotency markers and were positive for alkaline phosphatase activity (figure 3C,D). Following transduction, eGFP$^+$-sorted hiPSCs were expanded and used to form mesoderm-primed EBs, which can later shed the desired CAR-iMacs in a continuous manner (figure 3E). The CAR-iMacs production was sustained over several months (around 6 months) and provided consistent quality and quantities of iMacs ranging between 300,000 and 500,000 cells per well of a 6-well plate (figure 3F). CAR protein expression in terminally-differentiated iMacs was confirmed by immunoblot experiments to detect the CD8α hinge (figure 3H). The CAR expression did not alter the iMacs phenotype, as CAR-iMacs showed typical macrophage morphology and surface marker expression pattern, similar to eGFP or non-transduced control cells (eGFP or NTC) (figure 3G,I and online supplemental figure 3). Moreover, CAR-iMacs could successfully perform basic bacterial phagocytosis of *E. coli* bioparticles and secrete pro-inflammatory cytokines on subsequent challenge with LPS for 24 hours (figure 3J and online supplemental figures 2C,D and 3B).

CAR-iMacs showed enhanced phagocytosis and cytokine production on co-culture with CD19$^+$ Raji cells

To evaluate the CAR-mediated anticancer effects against CD19$^+$ target cells, CAR-expressing or control iMacs were co-cultured with CD19$^+$ mCherry-labeled Raji cells in a ratio of 1:1. After 4 hours, successful phagocytosis was shown by co-localization of Raji cells inside the CAR-iMacs as indicated by fluorescent microscopy and the image-based flow cytometry pictures (figure 4A–C). Phagocytic capacity was quantified via flow cytometry, analyzing the percentage of mCherry$^+$ iMacs. CAR-iMacs showed significantly higher levels of phagocytosis 52.26±6.88% compared with eGFP and NTC cells (16±1.62%, and 20.16±5.79%, respectively) (figure 4D). Furthermore, testing different effector/target ratios within the co-culture set-up showed an increase in phagocytosis of target cells, reaching up to 95% on proportional increase in target cell ratio (1:10) (online supplemental figure 3C). CAR-iMacs also demonstrated time-dependent phagocytosis, reaching almost 80% of phagocytosis after 8 hours of co-culture (figure 4E). Analyses of pro-inflammatory cytokine secretion showed higher secretion of IL-6 and significantly higher levels of TNF-α secretion from CAR-iMacs compared with the control cells when co-cultured with Raji cells (figure 4F,G).

CAR-iMacs performed antigen-specific phagocytosis of CD19$^+$ cancer cell lines and patient-derived acute lymphocytic leukemia cells

To investigate the antigen specificity of CAR-modified iMacs, we compared the macrophage phagocytic capacity against CD19^{low} or CD19$^+$ leukemia cell lines. Therefore, in addition to Raji cells, K562 (CD19^{low}) and Daudi (CD19$^+$) target cells were transduced with a monocistronic vector to express an mCherry reporter gene. Flow cytometric analyses showed similar levels of CD19 expression for Daudi and Raji cells, whereas K562 cells showed only low CD19 expression (figure 5A and online supplemental figure 3D). eGFP-expressing CAR or eGFP ctrl iMacs were co-cultured with mCherry$^+$ CD19$^{low/+}$ target cells in a ratio of 1:1, and, after 4 hours, the mCherry signal inside the CAR-iMacs was analyzed via flow cytometry. Whereas co-culture with CD19^{low} K562 cells led to low percentages of phagocytic macrophages for CAR-iMacs and eGFP$^+$ ctrl iMacs (average of 11.3% and 6.9%), CAR-iMacs demonstrated enhanced phagocytosis against CD19$^+$ Daudi cells and the highest increase of phagocytosis was observed against CD19$^+$ Raji cells (up to 43.0% and 75.9%, respectively) compared with eGFP ctrl macrophages that exhibited a substantially lower phagocytic capacity against both CD19$^+$ target cell lines (up to 13.1% and 34.7%, respectively) (figure 5B). This data is in line with the strength of CD19 expression on the target cells, indicating antigen specificity (figure 5A,B). Furthermore, analyses of TNF-α (figure 5C) and IL-6 (online supplemental figure 3E) secretion showed negligible TNF-α secretion from eGFP iMacs against all three target cell lines. Only CAR-iMacs showed a strong increase of TNF-α secretion when co-cultured with CD19$^+$ Daudi and Raji cells and only a slight increase against CD19^{low} K562 cells. Similar results were measured for IL-6 secretion, with CAR-iMacs showing a stronger secretion on co-culture with CD19$^+$ Daudi and Raji cells and less for CD19^{low} K562 cells. However, eGFP iMacs showed slight activity against Raji cells. To investigate whether the CAR also enhanced anticancer activity of iMacs against primary cancer cells, primary ALL samples from five different patients were investigated in co-culture experiments. Characterization of patient samples for purity, blast composition and CD19 expression showed that the ALL samples were of high purity with regard to B-cell composition with no presence of other contaminating cell types (online supplemental figure 4A,B). More than 80% of cells in four of the samples were CD19-positive, whereas one sample contained only 30% CD19-positive cells (figure 5D), which was used as negative control. Similarly to the observed effects with Raji cells, CAR-iMacs had enhanced phagocytosis of CD19$^+$

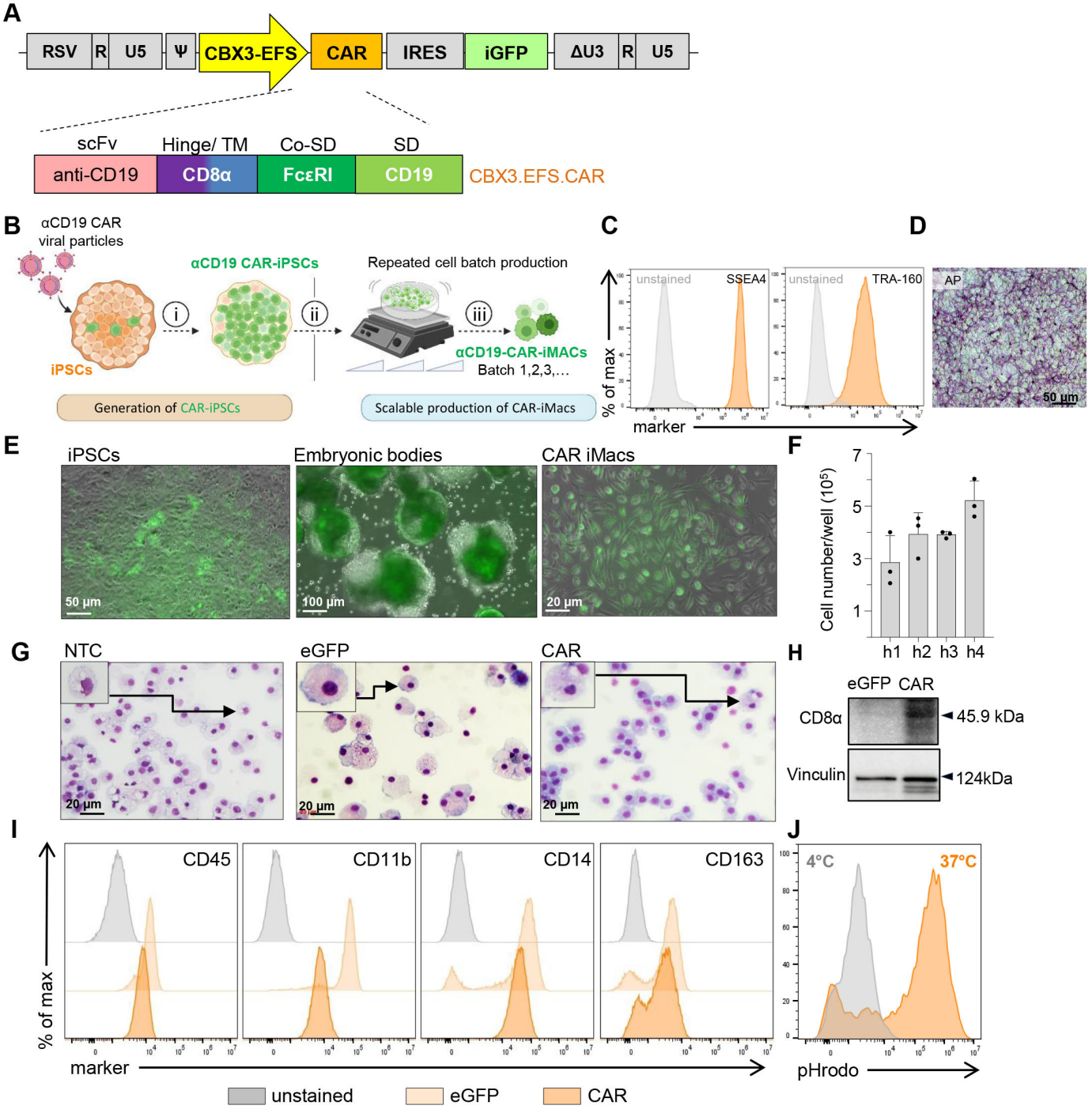

Figure 3 Characterization of anti-CD19 CAR-iPSCs and thereof derived CAR-iMacs. (A) CAR scheme demonstrating the composition of the subcloned anti-CD19 CAR (CAR). (B) Illustration of the work flow to generate CAR-iMacs. (C) Flow cytometry analyses of CAR hiPSC expression of SSEA4 and TRA160 in comparison to unstained controls. (D) Bright field microscopic images of alkaline phosphatase stained CAR hiPSCs (scale bar 50 µm). (E) Representative fluorescent microscopic images of the different steps of the hematopoietic differentiation of hiPSCs to iMacs. (F) Quantities of macrophages harvested from the supernatants at different weeks from various differentiation cultures (n=3 independent experiments, mean±SD). (G) Photographs of cytospins prepared from non-transduced iMacs (NTC), eGFP iMacs (eGFP), and the anti-CD19 CAR-iMacs (CAR) (scale bar 20 µm). (H) Western blot analysis of CD8α expression (45.9 kDa) in eGFP and CAR-iMacs, Vinculin (124 kDa) served as a control. (I) Flow cytometric analyses of macrophage surface markers (representative data of n=3, (online supplemental figure 3A)). (J) Analyses of pHrodo-*Escherichia coli* bioparticles phagocytosis via flow cytometry (representative data of n=5, (online supplemental figure 3B)). CAR, chimeric antigen receptor; Co-SD, co-stimulatory signaling domain;eGFP, enhanced green fluorescent protein expressing control iMacs; hiPSC, human induced pluripotent stem cell; scFv, single chain variable fragment; TM, transmembrane domain.

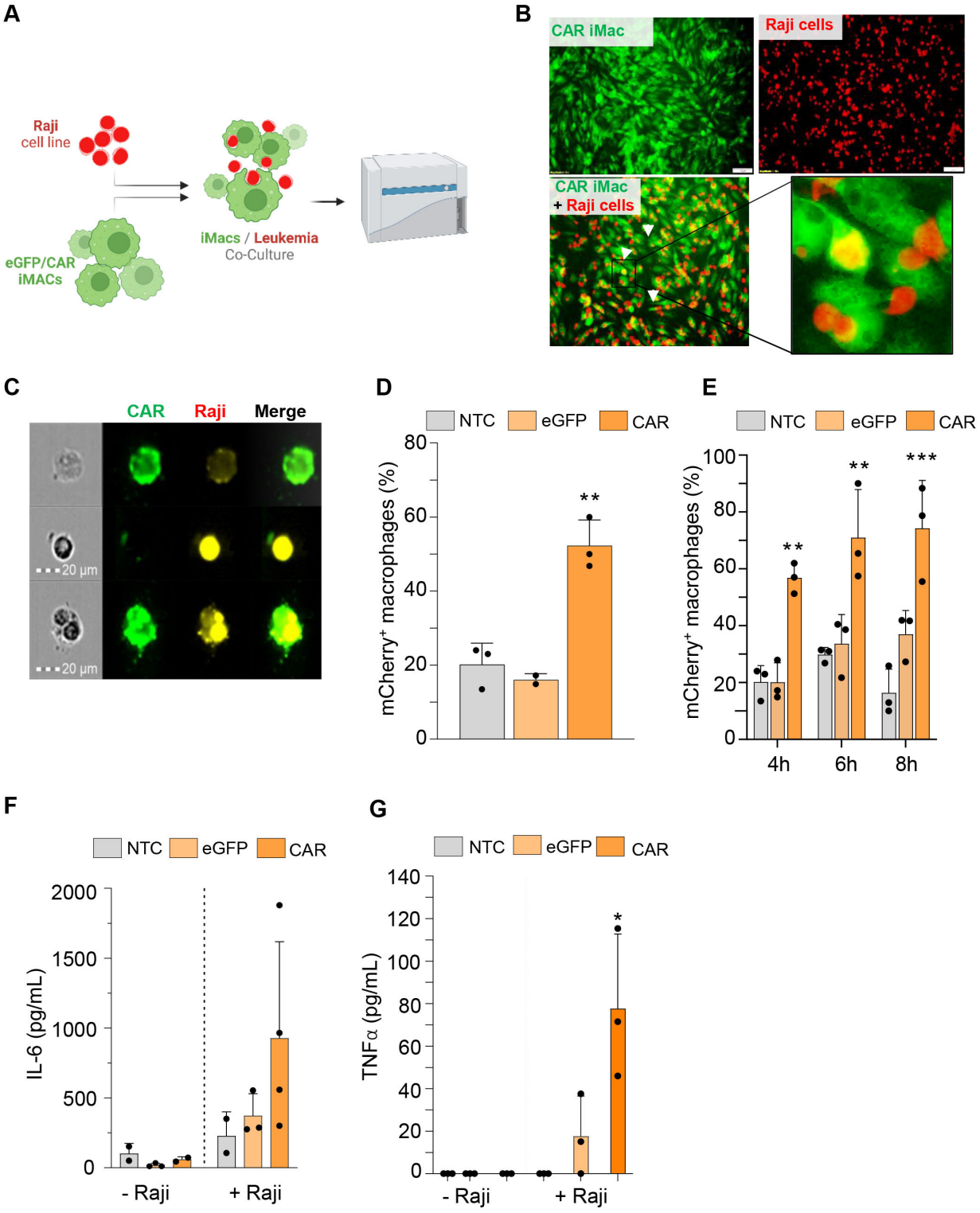

Figure 4 Assessment of CAR-mediated phagocytosis in human induced pluripotent stem cells-derived CAR-macrophages after co-culture with CD19⁺ Raji cells. (A) Schematic showing co-culture of CAR or eGFP iMacs with CD19⁺ Raji cells. (B) Representative fluorescent microscopic images of CAR-iMacs in co-culture with the target Raji cells (20×, scale bar: 20 µm). (C) Representative image from the acquired gallery using an image-based flow cytometer to analyze the co-localization of the target cells inside the co-cultured CAR-iMacs. (D) Flow cytometric analyses of percentage (%) of mCherry-positive Raji cells inside the eGFP⁺ macrophages (eGFP/CAR-iMacs) or the CD14 FITC stained non-transduced control cells (NTC) after co-culture with target cells for 4 hours or after increased incubation periods to 6 and 8 hours (E). ELISA assays of IL-6 (F) and TNF-α (G) secretion by the indicated iMacs in mono-cultures versus co-cultures with Raji cells. Data are represented as the mean±SD of n=2–3 biological replicates. Statistical significance was calculated with one-way analysis of variance using multiple comparisons. CAR, chimeric antigen receptor; eGFP, enhanced green fluorescent protein expressing control iMacs; IL, interleukin; TNF, tumor necrosis factor.

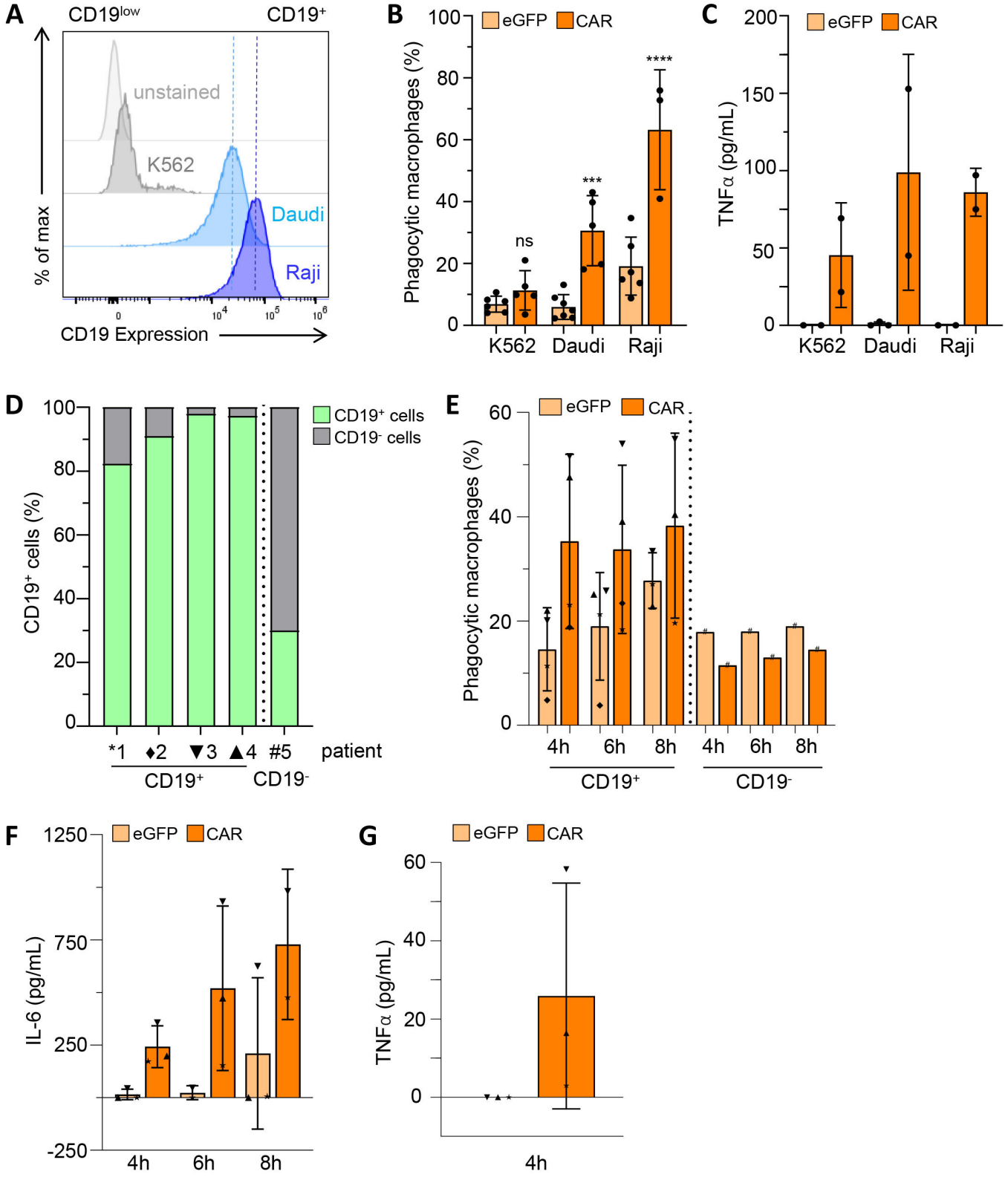

Figure 5 Assessment of CAR-mediated antigen specificity in iPSC-derived macrophages against CD19⁻ and patient with ALL samples. (A) MFI of CD19 expression on leukemia target cells (representative for n=2, (online supplemental figure 3D)). (B) Percentage (%) of phagocytic macrophages after 4 hours co-culture with CD19^{low} or CD19^{+} target cells. Statistical significance was calculated with one-way analysis of variance using multiple comparisons. (C) TNF-α secretion from iMacs after co-culture with target cells (n=2–3). (D) Percentage (%) of CD19 expression on cells from five different primary ALL patient samples. (E) Percentage (%) of phagocytic macrophages after co-culture with CD19^{low} or CD19^{+} primary ALL samples at the different indicated time points (n=4–5). ELISA assays of IL-6 (F) and TNF-α (G) secretion by the indicated iMacs after the co-culture with the different primary ALL samples (n=2–3). ALL, acute lymphocytic leukemia; CAR, chimeric antigen receptor; eGFP, enhanced green fluorescent expressing control iMacs; IL, interleukin; TNF, tumor necrosis factor.

ALL samples compared with control cells. This effect was seen in three out of the four CD19$^+$ ALL samples with highest phagocytosis levels of 54.9% after 8 hours (figure 5E). The observed phagocytosis of ALL samples by CAR-iMacs was also dependent on the CD19 antigen expression level, as there was no comparable phagocytosis increase when CAR-iMacs were co-cultured with the CD19^{low} control ALL sample (figure 5D,E). Additionally, CAR-iMacs secreted higher levels of IL-6 and TNF-α on co-culture with CD19$^+$ primary ALL samples compared with control cells (figure 5F,G).

CAR-iMacs show a pro-inflammatory phenotype and distinct gene expression to eGFP macrophages after co-culture with CD19$^+$ cancer cells

Macrophages exhibit strong plasticity and are able to adapt to various environmental stimuli such as cytokine secretion or cell-to-cell interaction. Thus, to further analyze the CAR-specific cell activation and underlying signaling pathways in detail, eGFP and CAR-macrophages were co-cultured with CD19$^+$ Raji cells or patient ALL samples, and subsequent scRNA-seq was performed (figure 6A). After merging and processing three scRNA data sets, we observed overlapping clusters in the UMAP analysis of two of the data sets. Notably, the UMAP representations revealed a similarity in the clustering patterns of CAR-macrophages, regardless of the target cells they were incubated with (CD19$^+$ Raji cells or patient ALL samples). In contrast, eGFP macrophages exhibited distinct clustering from the CAR-macrophage population, particularly following co-culture with CD19$^+$ Raji cells (figure 6B). Both eGFP-macrophages and CAR-macrophages exhibited typical macrophage markers (CD14, CD68, and CD163) (figure 6C). However, differential expression analysis revealed distinct expression patterns in expressed genes between the two groups (figure 6D, online supplemental figure 5A). Comparing the enriched GO terms in biological processes for the top 200 differentially expressed genes, it became evident that CAR-iMacs exhibited a more pronounced activation of antiviral response and cytokine-mediated responses. In contrast, eGFP macrophages demonstrated activation of general cellular processes, including chemotaxis, migration, and cell differentiation pathways (online supplemental figure 5B). When focusing on function-associated genes, CAR-macrophages exhibited significant upregulation of pro-inflammatory-related genes, including interferon-associated genes, co-stimulatory genes (CD80 and CD40), and chemokines involved in attracting immune cells (CCL5 and CCL2) (figure 6E,F). Notably, CAR-macrophages also displayed increased gene expression associated with antigen presentation within the context of major histocompatibility complex (MHC)-I and MHC-II, accompanied by the induction of Nuclear factor kappa B (NF-κB) signaling (figure 6G,H). These findings indicate CAR-specific cell activation, demonstrating their superior ability to transition into a potent M1 phenotype. This activation enables them to effectively recruit additional immune cells in the battle against cancer cells.

To further explore CAR-macrophages, we focused on the Louvain clustering and trajectory inference analysis. The results revealed distinct temporal changes, with a pro-inflammatory-activated M1 phenotype (cluster 0) and transitioning towards a less-activated and more pro-resolution phenotype (cluster 1). This transition was supported by the dynamic expression patterns of key genes, such as RARRES1 in cluster 0 and IGF2BP2 in cluster 1 (figure 6I). Additionally, across both eGFP and CAR-iMacs samples, there seems to be a distinct differential expression of pro-inflammatory and anti-inflammatory marker genes, with higher expression of RARRES1 and HLA-DR within the CAR-macrophage cluster 0, overlapping with the observed higher activation in phagocytic activity between eGFP and CAR-iMacs after 4 hours of co-culture (online supplemental figure 5C).

Continuous upscaled production of functional CAR-iMacs using a bioreactor system

While the production of CAR-iMacs from iPSCs was shown before with classical two dimensional systems, the upscaled three dimensional production of genetically-modified macrophages is a novel advance. Thus, we used an upscaling, automated CERO 3D bioreactor, where CAR-iPSCs were differentiated to CAR-iMacs using a continuous suspension differentiation protocol (figure 7A). The weekly yield of harvested CAR-iMacs increased over time and attained a stable production of up to ~5.73×10^7 cells/40 mL (figure 7B). The CAR-iMacs displayed a typical macrophage morphology (figure 7C) and phenotype (figure 7D). Additionally, the produced CAR-iMacs were of consistent quality, purity and functionality providing mature CAR-iMacs with every harvest (figure 7E,F). The generated CAR-iMacs also maintained their antigen-dependent functionality against CD19$^+$ target cells by exhibiting the highest phagocytic capacity against CD19$^+$ Raji and Daudi cells and a much lower phagocytic activity against CD19^{low} K562 cells (figure 7G). It is worth noting, that irrespective of the manufacturing method, the generated CAR-iMacs continued to display a comparable phagocytic activity against CD19$^+$ Raji target cells (online supplemental figure 6E). Furthermore, in a combined co-culture of CD19$^+$ Raji and CD19^{low} K562 cells, only CAR-iMacs led to a decrease of CD19$^+$ Raji cells, reaching 50% Raji cells after 48 hours of co-culture compared with eGFP iMacs, confirming successful elimination of target cells (online supplemental figure 6F). Additionally, CAR-iMacs showed higher secretion levels of pro-inflammatory cytokines and chemokines (IL-6, TNF-α, IL-1β, IL-1RA and Interferon gamma-induced protein 10(IP-10)) upon co-culture with CD19$^+$ Raji cells compared with eGFP iMacs (figure 7H,I and online supplemental figure 6A–C). Moreover, peripheral blood-derived primary T cells demonstrated a stronger activation after incubation with supernatants from CAR-iMacs and CD19$^+$Raji co-cultures, showing a significantly-higher

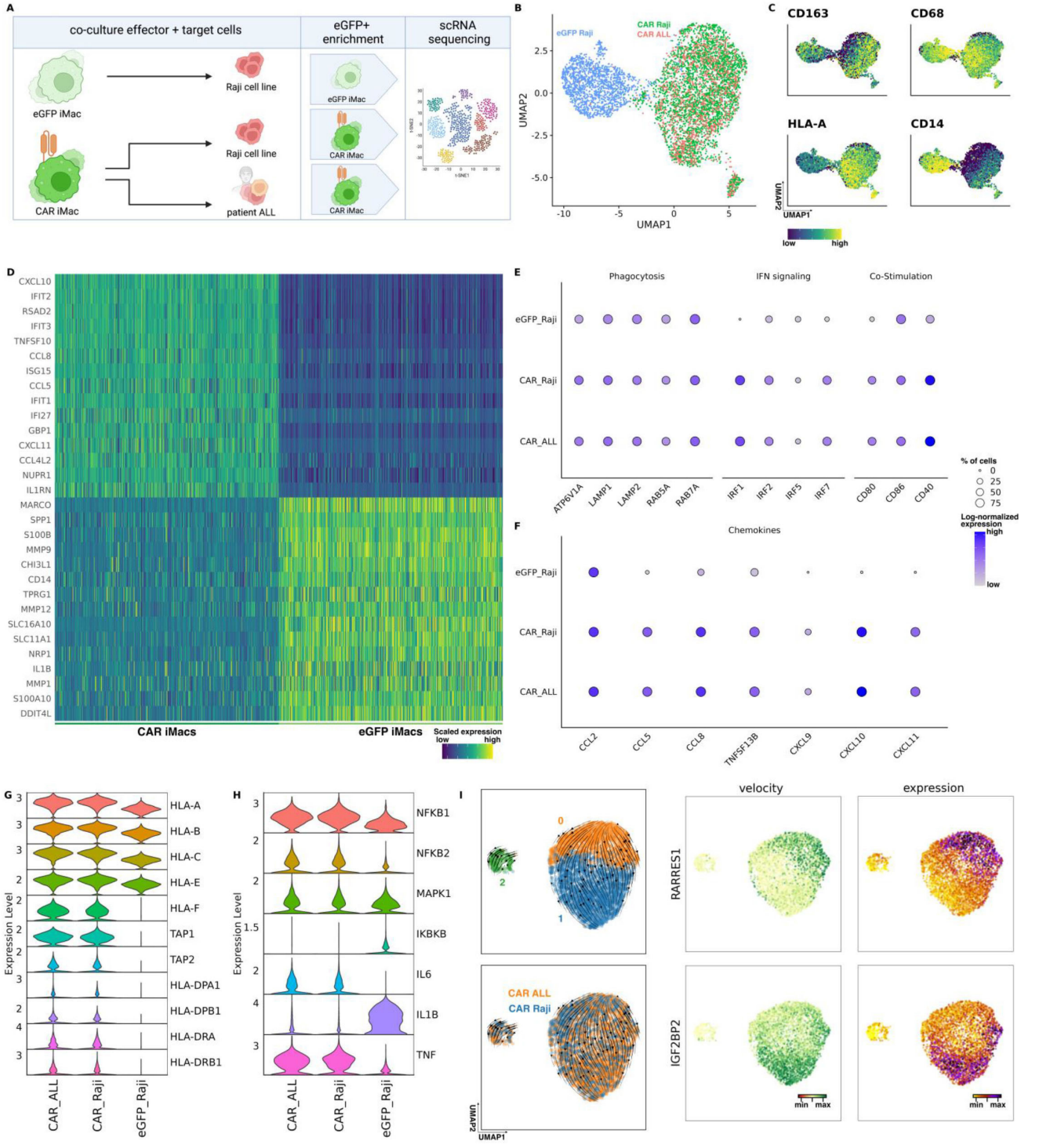

Figure 6 CAR-iMacs show pro-inflammatory phenotype after co-culture with CD19⁺ target cells. (A) Scheme showing co-culture of CAR-iMacs or eGFP-iMacs with CD19⁺ Raji cells or ALL patient samples followed by subsequent scRNA-seq analysis. (B) UMAP plots illustrating the phenotypic distinction of eGFP-macrophages and CAR-macrophages after co-culture with CD19⁺ Raji or ALL cells colored according to cell lineages. (C) UMAP plots of CAR-macrophages and eGFP-macrophages after culturing with CD19⁺ Raji cells, showing the relative expression of typical macrophage genes within the populations colored according to gene expression. (D) Top 15 differentially-expressed genes of CAR-macrophage population after co-culture with Raji or ALL cells compared with eGFP-macrophage population. (E) and (F) Clustered dot plots showing differentially-expressed genes of eGFP-macrophages and CAR-macrophages after co-culture with Raji cells. (G) and (H) Violin plots illustrating differentially-expressed genes in eGFP-macrophages and CAR-macrophages in the context of antigen presentation and NF-κB signaling. (I) RNA velocity analysis and representative gene expression showing the progression of subsets inside the CAR-macrophage population. ALL, acute lymphocytic leukemia; CAR, chimeric antigen receptor;eGFP, enhanced green fluorescent expressing control iMacs; NF-κB, nuclear factor kappa B; scRNA-seq, single-cell RNA sequencing; UMAP, Uniform Manifold Approximation and Projection.

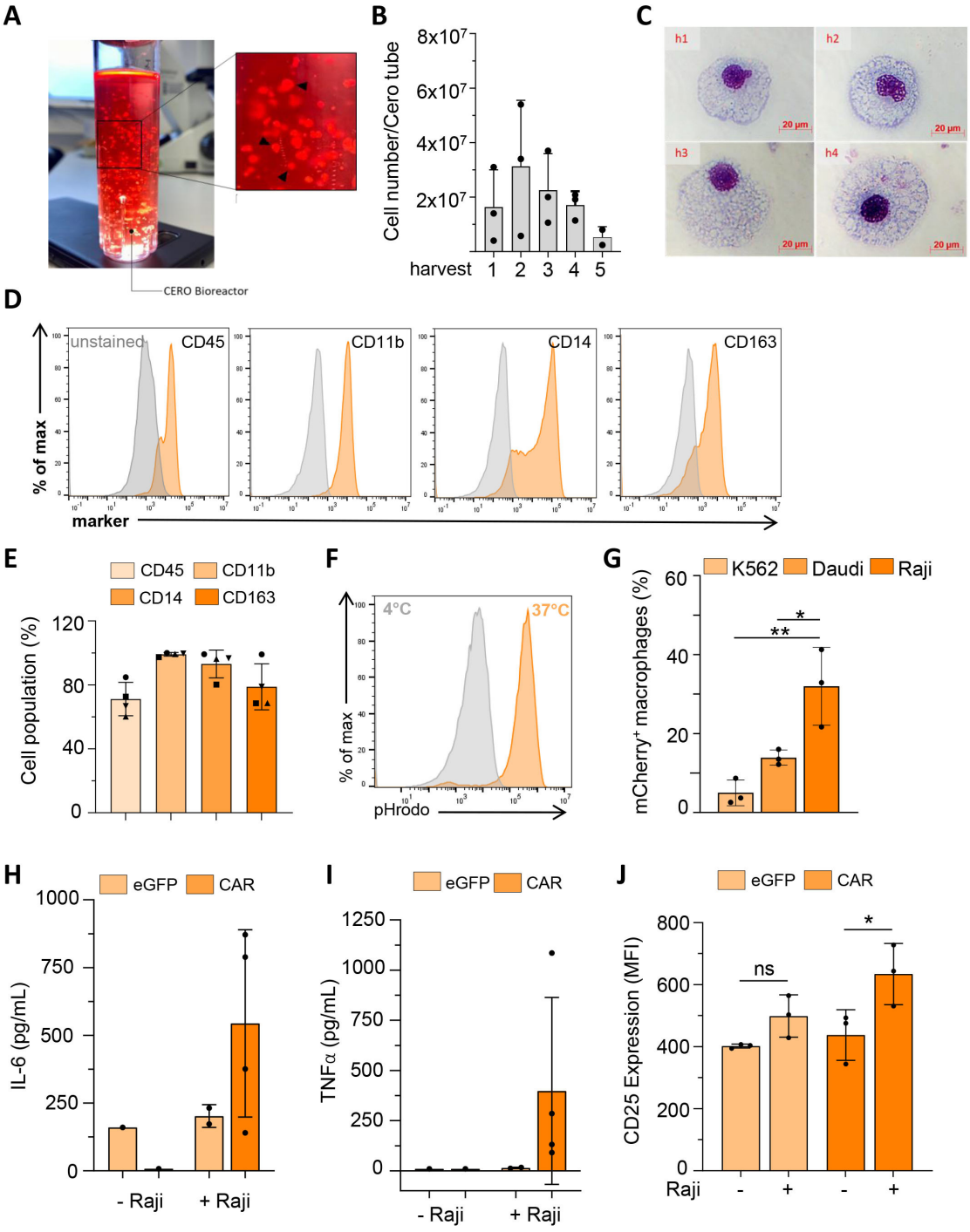

Figure 7 Continuous upscaled production of CAR-iMacs in a CERO bioreactor. (A) Photo illustrating the ongoing differentiation of anti-CD19 CAR-induced pluripotent stem cells in the 50 mL bioreactor tube, highlighting the formation of the hemanoids, which are continuously shedding the CAR-iMacs. (B) Quantities of CAR-iMacs harvested from the supernatants at different weeks from the ongoing bioreactor differentiation (n=3). (C) Representative cytospin images of the generated CAR-iMacs from every harvest. (D) Histograms of the flow cytometric analysis of macrophage surface markers compared with unstained control cells, (representative data of n=4, (online supplemental figure 6D)). (E) Bar chart quantifying the percentage (%) of surface marker expression from the stained CAR-iMacs from every harvest (different symbols reflect different harvests). (F) Flow cytometry analysis of pHrodo-*Escherichia coli* bioparticle phagocytosis by iMacs, (representative data of n=5, (online supplemental figure 3B)). (G) Bar chart quantifying the phagocytosis of mCherry$^+$-labeled target cells inside the GFP$^+$ CAR-iMacs via flow cytometry. LEGENDplex analysis of (H) IL-6 and (I) TNF-α secretion by CERO-bioreactor-generated iMacs in mono-cultures versus co-cultures with Raji cells. (J) Flow cytometric analyses of T-cell activation (CD25 expression) after 24 hours of incubation with supernatants from co-cultures (eGFP/CAR-iMacs and Raji cells for 4 hours). Data are represented as the mean±SD of n=3–4 biological replicates. Statistical significance was calculated with one-way analysis of variance using multiple comparisons. CAR, chimeric antigen receptor;eGFP,enhanced green fluorescent protein expressing control iMacs; IL, interleukin; MFI, mean fluorescence intensity; TNF, tumor necrosis factor.

increase in CD25 expression (figure 7J) and increased CD69 expression (online supplemental figure 6G), in comparison to supernatants from eGFP control iMacs. Furthermore, CAR-iMacs revealed a higher capacity to retain their pro-inflammatory phenotype after exposure to immunosuppressive conditions (dexamethasone), highlighting a stable expression of CD86 (pro-inflammatory marker) and stable secretion of TNF-α, in comparison to a decreased TNF-α secretion by eGFP iMacs (online supplemental figure 6H and I). In summary, the reported results demonstrated the feasibility of adapting the iMac differentiation protocols to different upscaling platforms, while maintaining the functionality and phenotype of the genetically-modified iMacs.

DISCUSSION

To overcome profound challenges associated with the manufacturing and applicability of CAR-macrophages, we here introduced the generation of functional and antigen-specific CAR-macrophages using cord blood-derived $CD34^+$ HSPCs and human iPSCs as stem cell sources. The unique manufacturing regimen to continuously produce human macrophages from iPSCs in scalable quantities was used as a proof-of-concept, demonstrating its suitability in the context of $CD19^+$ leukemia. We first showed CAR-modified HSPCs exhibiting persistent transgene expression after differentiation into human CAR-macrophages, successful targeting and a pro-inflammatory response following co-culture with $CD19^+$ cancer cells. These results are in agreement with a previous study that showed successful generation of anti-CEA CAR-macrophages from cord blood-derived HSPCs.[14] However, the use of cord blood for the derivation of CAR-macrophages is suboptimal due to limited availability of suitable donors for cord blood samples alongside the low yields of $CD34^+$ cells. Thus, most studies rely on the derivation of peripheral blood monocytes, which have similar drawbacks. In the present study, we used hiPSCs to generate scalable numbers of anti-CD19 CAR-macrophages. In fact, iPSCs offer numerous advantages over other stem cell types that make them a great candidate for CAR-macrophage production. Besides the seminal feature of iPSCs to be maintained in long-term culture and expanded almost indefinitely due to self-renewal capacity, they are highly susceptible for genetic modification and show clonal and genetic stability, thus, avoiding donor-to-donor variability. Furthermore, different attempts to generate, for example, hypoimmunogenic iPSC-derivatives, HLA-homozygous iPSCs or other forms of "stealth" iPSCs offer new options to combine the CAR technology with modern iPSC concepts to establish allogenic cell products for next generation cell-based immunotherapies. Previous studies revealed the successful generation of functional CAR-iMacs targeting leukemia or solid tumors, using an anti-GD2 CAR,[22] or an anti-mesothelin CAR with a CD3ζ signaling domain,[23] respectively. However, silencing of the CAR transgene was reported to be a major hurdle and is a typical problem when it comes to the use of pluripotent stem cells.[23] Hence, to ensure stable gene expression in hiPSCs, we used an elongation factor short promoter together with the ubiquitous chromatin opening CBX3 element, which was previously shown to reduce epigenetic methylation.[24] This approach enabled us to produce iMacs with stable CAR expression in repetitive harvests. Using this unique technology, we were also able to use feeder-free and serum-free culture conditions as well as a scalable differentiation system. CD19-CAR-iMacs showed specific anticancer functionality, promoting a time-dependent and antigen-dependent phagocytosis of $CD19^+$ target cells, while only background phagocytosis was observed with $CD19^{low}$ leukemia cells. In addition, the CAR construct facilitated a pro-inflammatory microenvironment that was independent of the target cell type. In fact, scRNA-seq revealed the same behavior and repolarization of CAR-iMacs post co-culture with Raji or primary $CD19^+$ patient with ALL samples, highlighting the specificity of the CAR construct and new insights into the mode of action of the CAR. The proposed mechanisms are in line with previous studies that demonstrate a reprograming of the TME towards an inflammatory milieu,[8 23] which is most likely driven by the CAR-mediated signaling activity. As of yet, the efficacy of CAR-iMacs was evaluated primarily against cancer cell lines and murine models. Taking a clear step forward, we demonstrate the functionality of CAR-iMacs against clinical samples from patients with ALL, showing that CAR-iMacs can eradicate $CD19^+$ blasts within primary ALL samples. scRNA-seq analysis upon co-culture with target cells gave further insights into the CAR-iMac signaling pathways, demonstrating a similar pattern of immune responses regardless of the $CD19^+$ target cell type, including a strong activation and polarization towards a pro-inflammatory M1 phenotype with interferon signaling and the upregulation of chemokines and co-stimulatory genes, indicating the possibility of a potential interaction with additional immune cells. Moreover, subclustering of CAR-iMacs revealed a switch towards an anti-inflammatory M2 phenotype, indicating controlled regulation of anticancer immune responses. Additionally, compared with eGFP iMacs, the CAR-iMacs showed a strong antiviral immune response upon activation, which was shown to further enhance antitumor immunity via activation of interferon pathways.[25]

Furthermore, iPSCs can also be rigorously tested with respect to safety issues. Once safety and efficacy are established and iPSC therapeutics are approved, master and working cell-banks can be generated for future upscaling approaches. The latter is an important issue and currently limits the broad applicability of CAR-macrophages. Additionally, it is known that high doses of cell-based therapies are often necessary to achieve the desired therapeutic efficacy. For instance, tisagenlecleucel, a Food and Drug Administration (FDA) approved CAR T-cell therapy, is indicated at doses ranging between 60 and 600 million cells.[26] Providing such quantities of primary immune cells from often immune-compromised patients can be a major

hurdle. To generate these numbers of CAR-macrophages, we introduced the use of a scalable, three-dimensional suspension-based differentiation system, which can be used for the transition into more sophisticated bioreactors. To derive CAR-iMacs, an automated CERO 3D bioreactor was used, highlighting the overall feasibility to perform upscaling approaches. Given previous attempts employing industry compatible 250 mL bioreactors and differentiation schemes, which are fully defined, clearly demonstrates the overall potential of human iPSC-derived macrophages. Hence, our proof-of-concept using the demonstrated intermediate upscaling of CAR-iMacs with the CERO bioreactor can be further adapted to the industry-compliant bioreactor platform. This is particularly essential in the context of cell-based therapy, as it is known that high doses are indicated to achieve the needed therapeutic effect. Overall, the presented work showcase an innovative scalable and continuous platform exploiting the unlimited regenerative features of stem cells, while providing a translational clinical access to CAR-macrophage therapeutics. Additionally, it is noteworthy that the iPSC platform can provide a valuable tool revealing novel insights into the molecular pathways and mechanism driving the CAR mediated anticancer response.

Author affiliations
[1]Department of Pediatric Pneumology, Allergology and Neonatology, Hannover Medical School, Hannover, Germany
[2]Center for Translational and Regenerative Medicine, Hannover Medical School, Hannover, Germany
[3]Department of Hematology, Hemostasis, Oncology and Stem Cell Transplantation, Hannover Medical School, Hannover, Germany
[4]Fraunhofer Institute for Toxicology and Experimental Medicine ITEM, Hannover, Germany
[5]Institute of Experimental Hematology, Hannover Medical School, Hannover, Germany
[6]Institute of Transplant Immunology, Hannover Medical School, Hannover, Germany
[7]Department of Obstetrics and Gynecology, Hannover Medical School, Hannover, Germany
[8]Division of Hematology/Oncology, Boston Children's Hospital, Harvard Medical School, Boston, Massachusetts, USA
[9]RESIST, Cluster of Excellence, Hannover Medical School, Hannover, Germany

Acknowledgements The authors would like to acknowledge the laboratory of Ronald D vale for depositing their CD19-targeting lentivirus vector in the addgene repository, which was used in the presented work.

Contributors Conceptualization: SMA, DP, NL, MM, AS, TM. Methodology development: DP, SMA, MM, MCO, M-SJ, NL. Data acquisition: SMA, DP, MCO, M-SJ, PJM, ASt, MA. Analysis and interpretation of data: SMA, DP, M-SJ, MCO, ASc, MA. Original draft preparation: DP, SMA, MCO, M-SJ, NL. Revision: DP, SMA, M-SJ, MA, ASt, NL. Study supervision: MM, TM, NL. Funding acquisition: NL, MM and GH. All authors have reviewed and commented on the submitted manuscript.

Funding This project has received funding from the European Research Council (ERC) under the European Union's Horizon 2020 research and innovation program (grant agreement No. 852178 and grant agreement No. 101100859 "iPYRO"). The work is also funded by the Deutsche Forschungsgemeinschaft (DFG, German Research Foundation) under Germany's Excellence Strategy - EXC 2155 - project number 390874280 and REBIRTH Research Center for Translational Regenerative Medicine "Förderung aus Mitteln des Niedersächsischen Vorab" (grant: ZN3340).

Competing interests NL, MA and TM have filled a patent application on the generation of human iPSC-derived macrophages. All other authors declare no conflict of interest.

Patient consent for publication Not applicable.

Ethics approval This study involves human participants and was approved by Hannover Medical School Ethics Committee (protocol code 1303-2012). This study involves human patient samples (ethical numbers 666/2010 and 3639_2017). Participants gave informed consent to participate in the study before taking part.

Provenance and peer review Not commissioned; externally peer reviewed.

Data availability statement Data are available upon reasonable request. All data relevant to the study are included in the article or uploaded as supplementary information.

ORCID iDs
Daniela Paasch http://orcid.org/0009-0002-6857-8784
Nico Lachmann http://orcid.org/0000-0002-4245-1497

REFERENCES

1 Pan K, Farrukh H, Chittepu VCSR, *et al*. CAR race to cancer Immunotherapy: from CAR T, CAR NK to CAR macrophage therapy. *J Exp Clin Cancer Res* 2022;41:119.
2 Williams BA, Law AD, Routy B, *et al*. A phase I trial of NK-92 cells for refractory hematological malignancies relapsing after autologous hematopoietic cell transplantation shows safety and evidence of efficacy. *Oncotarget* 2017;8:89256–68.
3 Albinger N, Hartmann J, Ullrich E. Current status and perspective of CAR-T and CAR-NK cell therapy trials in Germany. *Gene Ther* 2021;28:513–27.
4 Wagner J, Wickman E, DeRenzo C, *et al*. CAR T cell therapy for solid tumors: bright future or dark reality? *Mol Ther* 2020;28:2320–39.
5 Wrona E, Borowiec M, Potemski P. CAR-NK cells in the treatment of solid tumors. *Int J Mol Sci* 2021;22:5899.
6 Tang-Huau T-L, Gueguen P, Goudot C, *et al*. Human in vivo-generated monocyte-derived dendritic cells and macrophages cross-present antigens through a vacuolar pathway. *Nat Commun* 2018;9:2570.
7 Mantovani A, Allavena P, Marchesi F, *et al*. Macrophages as tools and targets in cancer therapy. *Nat Rev Drug Discov* 2022;21:799–820.
8 Klichinsky M, Ruella M, Shestova O, *et al*. Human Chimeric antigen receptor macrophages for cancer immunotherapy. *Nat Biotechnol* 2020;38:947–53.
9 Morrissey MA, Williamson AP, Steinbach AM, *et al*. Chimeric antigen receptors that trigger Phagocytosis. *Elife* 2018;7:e36688.
10 Abdin SM, Paasch D, Morgan M, *et al*. Cars and beyond: Tailoring macrophage-based cell Therapeutics to combat solid malignancies. *J Immunother Cancer* 2021;9:e002741.
11 Ackermann M, Rafiei Hashtchin A, Manstein F, *et al*. Continuous human iPSC-macrophage mass production by suspension culture in stirred tank Bioreactors. *Nat Protoc* 2022;17:513–39.
12 Takata K, Kozaki T, Lee CZW, *et al*. Induced-Pluripotent-stem-cell-derived primitive macrophages provide a platform for modeling tissue-resident macrophage differentiation and function. *Immunity* 2017;47:183–98.
13 Douthwaite H, Arteagabeitia AB, Mukhopadhyay S. Differentiation of human induced Pluripotent stem cell into Macrophages. *Bio Protoc* 2022;12:e4361.
14 Paasch D, Meyer J, Stamopoulou A, *et al*. Ex vivo generation of CAR macrophages from hematopoietic stem and progenitor cells for use in cancer therapy. *Cells* 2022;11:994.
15 Beneke V, Küster F, Neehus A-L, *et al*. An immune cell spray (ICS) formulation allows for the delivery of functional monocyte/macrophages. *Sci Rep* 2018;8:16281.

16 Hao Y, Hao S, Andersen-Nissen E, *et al*. Integrated analysis of multimodal single-cell data. *Cell* 2021;184:3573–87.
17 McGinnis CS, Murrow LM, Gartner ZJ. Doubletfinder: doublet detection in single-cell RNA sequencing data using artificial nearest neighbors. *Cell Syst* 2019;8:329–37.
18 Wu T, Hu E, Xu S, *et al*. clusterProfiler 4.0: A universal enrichment tool for interpreting Omics data. *Innovation (Camb)* 2021;2:100141.
19 La Manno G, Soldatov R, Zeisel A, *et al*. RNA velocity of single cells. *Nature* 2018;560:494–8.
20 Bergen V, Lange M, Peidli S, *et al*. Generalizing RNA velocity to transient cell States through dynamical modeling. *Nat Biotechnol* 2020;38:1408–14.
21 Andreesen R, Scheibenbogen C, Brugger W, *et al*. Adoptive transfer of tumor cytotoxic macrophages generated in vitro from circulating blood monocytes: a new approach to cancer Immunotherapy. *Cancer Res* 1990;50:7450–6.
22 Zhang J, Webster S, Duffin B, *et al*. Generation of anti-Gd2 CAR macrophages from human pluripotent stem cells for cancer immunotherapies. *Stem Cell Reports* 2023;18:585–96.
23 Zhang L, Tian L, Dai X, *et al*. Pluripotent stem cell-derived CAR-macrophage cells with antigen-dependent anti-cancer cell functions. *J Hematol Oncol* 2020;13:153.
24 Müller-Kuller U, Ackermann M, Kolodziej S, *et al*. A minimal ubiquitous chromatin opening element (UCOE) effectively prevents silencing of juxtaposed heterologous promoters by epigenetic remodeling in multipotent and Pluripotent stem cells. *Nucleic Acids Res* 2015;43:1577–92.
25 Vitiello GAF, Ferreira WAS, Cordeiro de Lima VC, *et al*. Antiviral responses in cancer: boosting antitumor immunity through activation of interferon pathway in the tumor Microenvironment. *Front Immunol* 2021;12:782852.
26 Rotte A, Frigault MJ, Ansari A, *et al*. Dose-response correlation for CAR-T cells: a systematic review of clinical studies. *J Immunother Cancer* 2022;10:e005678.